



# LIQUEFACTION-INDUCED GROUND DISPLACEMENTS IN UCHINADA TOWN BY THE 2024 NOTO PENINSULA EARTHQUAKE

Akio SAKAMOTO<sup>1</sup> and Masanori HAMADA<sup>2</sup>

<sup>1</sup> Member, Dr. Eng., Technical Advisor, Institute for Disaster Mitigation of Industrial Complexes, Kanagawa, Japan, sakamoto\_akio@outlook.jp

<sup>2</sup> Honorary Member, Dr. Eng., Representative Director, Institute for Disaster Mitigation of Industrial Complexes, Kanagawa, Japan, hamada@waseda.jp

**ABSTRACT:** The 2024 Noto Peninsula Earthquake on January 1, 2024, caused extensive ground damage, including landslides and liquefaction. In Uchinada Town, Ishikawa Prefecture, which is located on the sand dunes, liquefaction caused large ground displacements with sand boils, fissures, subsidence and uplift. Roads, lifelines, buildings and houses were severely damaged. The authors measured the ground displacements by 3D survey using aerial photographs and discussed the effect of surface gradient on the displacements.

**Keywords:** *The 2024 Noto Peninsula Earthquake, Liquefaction, Ground displacement, Sand dune, Aerial photograph*

## 1. INTRODUCTION

Uchinada Town, the survey area, is located on sand dunes. In the gently sloping low-elevation section on the east side of the sand dunes, the liquefaction-induced ground displacements occurred. Fissures, subsidence, and uplift were observed on the surface, causing damage to roads, buried lifeline pipes, and buildings. The authors identified ground failures, such as sand boils and fissures, and measured ground displacements using pre- and post-earthquake aerial photographs of Uchinada Town<sup>1)</sup>. The report presents some of the findings from the survey.

## 2. THE 2024 NOTO PENINSULA EARTHQUAKE AND DAMAGE IN UCHINADA TOWN

In Uchinada Town, located about 100 km away from the epicenter of the Noto Peninsula Earthquake (Mj 7.6), a seismic intensity V– in JMA (Japan Meteorological Agency Scale) and a maximum acceleration (3 components composed) of more than 190 cm/s<sup>2</sup> were observed<sup>2), 3)</sup>. The liquefaction in Uchinada Town occurred in low-elevation sections that are situated under the eastern steep slopes of the dune ridge line extending from north to south. Liquefied ground moved along the sloping direction, inducing fissures, subsidence, and uplift. Road pavements were impassable due to fissures, subsidence, and uplift, buried lifeline pipes lost functionality for extended periods due to deformation and damage,

and numerous residential buildings suffered from subsidence, inclination, and collapse.

The authors surveyed these ground failures and damage to facilities in the field on February 20, 2024 and July 15–16, 2024. According to official reports as of March 6, 2025, a total of 124 houses were completely destroyed and 564 were partially damaged in Uchinada Town<sup>4)</sup>.

### 3. TOPOGRAPHY OF UCHINADA TOWN AND SURVEY AREA

#### 3.1 Topography

Figure 1 shows the topography of Uchinada Town. Figure 1(a) is a map of the town including the surrounding areas. The town is located along the Sea of Japan, and the main part of the town is mostly situated on the Uchinada Sand Dunes<sup>5), 6)</sup>. The formation of the sand dunes began in the Jomon period, a prehistoric cultural era in Japan. Sediment discharged into the Sea of Japan by Tedoru River and other rivers was carried to the land area by strong sea breezes, forming sandbar-shaped sand dunes. As a result, the water area of Lake Kahokugata, a shallow lagoon, was left on the inland side<sup>7)</sup>. Due to the national reclamation project that began in the 1960s, the surface area of the lagoon is now 1/3 of its original area. Reclaimed land extends over the eastern side of the northern area of Uchinada Town. Figures 1(b) and 1(c) show cross-sectional views of the topographical changes in Uchinada Town.

In the northern area, lagoon was filled with soil excavated from the eastern slope of the dunes, resulting in steep slopes and excavation sites were formed. The excavation sites were later replaced by farmlands and residential areas. Figure 1(b) shows the topography of Nishiaraya District, which was particularly heavily damaged in the northern area. On the other hand, the southern area was developed for housing construction early on due to its nearby location to Kanazawa City. Figure 1(c) shows the topography of Tsurugaoka District, which showed relatively heavy damage in the southern area. This

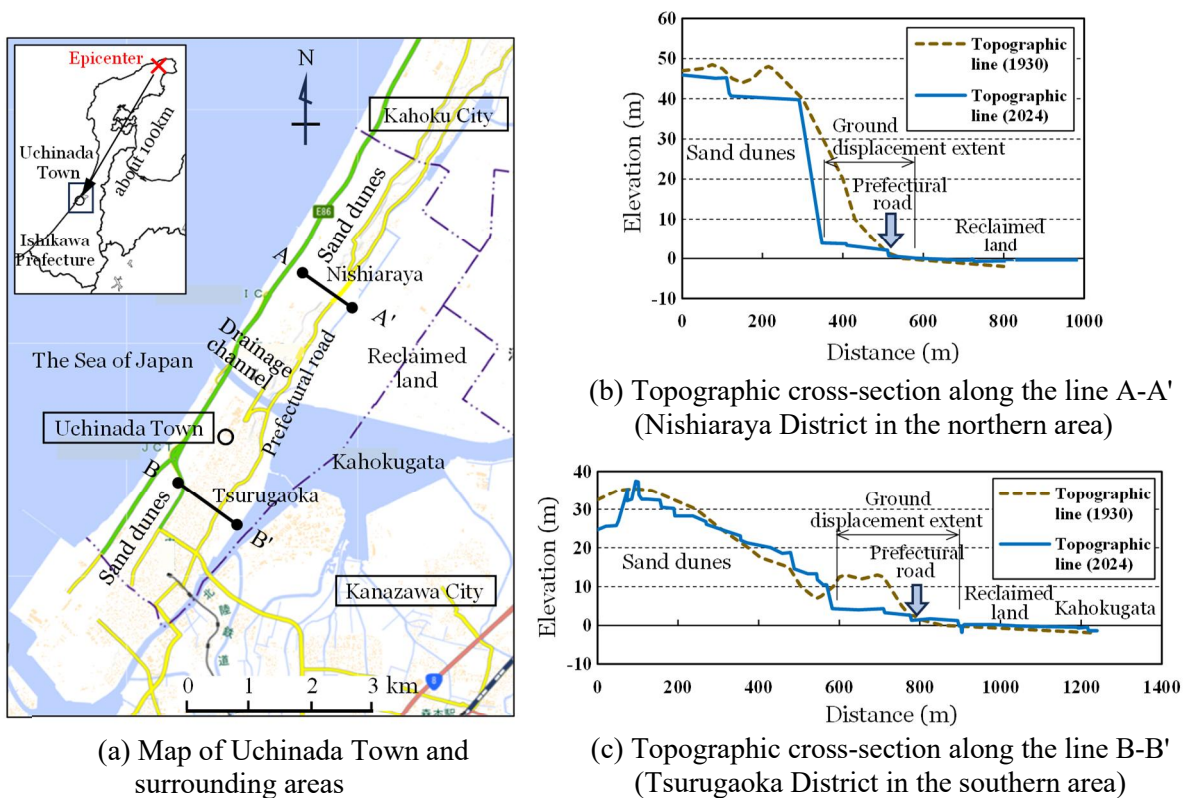


Fig. 1 Topography of Uchinada Town<sup>1)</sup>

area has residential zones extending from the top of the sand dunes to the reclaimed land facing Lake Kahokugata. As shown in Figs. 1(b) and 1(c), the cross section in 1930 is drawn based on a 1:25,000 topographic map<sup>8), 9)</sup>, and the cross section in 2024 is drawn based on post-earthquake aerial photogrammetric data, as described later.

### 3.2 Resources used for the survey

Table 1 shows the resources used for the survey. In the table, (1) to (4) are existing resources. (5) are aerial photos taken 70 days after the earthquake, by Institute for Disaster Mitigation of Industrial Complexes, Kanagawa, Japan. Although several days had passed since the earthquake, ground failures of a certain size could still be discerned in these photos. The aerial photos shown in (2) and (3), of Nishiaraya (taken in 2012) and Tsurugaoka (taken in 2007), respectively, were taken about 12 and 17 years before the earthquake. It was considered that some facilities had been artificially altered during this period. Therefore, we compared (2) and (3) with satellite photos taken just before the earthquake (taken in 2023) in (4). As a result, renewal of roads and irrigation channels and reconstruction of buildings were observed, and these were excluded from the targets (observation points) for reading the coordinates.

Table 1 Resources used for the survey

No.	Resources	Publisher	Date	Specification	Purposes
(1)	Topographic map of Uchinada Town (1:2,500) <sup>10)</sup>	Uchinada Town Office	Surveyed in 2016.	Digital topographic map in DM format	<ul style="list-style-type: none"> <li>• Selection of control points and extraction of the coordinates</li> <li>• Background for ground failure maps and ground displacement maps</li> </ul>
(2)	Pre-earthquake aerial photos (Nishiaraya District) <sup>11)</sup>	Geospatial Information Authority of Japan	Taken in 2012.	20 μm resolution	<ul style="list-style-type: none"> <li>• Measurement of ground displacements</li> </ul>
(3)	Pre-earthquake aerial photos (Tsurugaoka District) <sup>12)</sup>	Geospatial Information Authority of Japan	Taken in October 2007.	20 μm resolution	<ul style="list-style-type: none"> <li>• Measurement of ground displacements</li> </ul>
(4)	Pre-earthquake satellite photos (Nishiaraya, Tsurugaoka)	Google Earth	Taken on August 12, 2023.		<ul style="list-style-type: none"> <li>• Identification of ground failures</li> </ul>
(5)	Post-earthquake aerial photos (Nishiaraya, Tsurugaoka)	Institute for Disaster Mitigation of Industrial Complexes, Japan	Taken on March 11, 2024.	20 μm resolution	<ul style="list-style-type: none"> <li>• Identification of ground failures</li> <li>• Measurement of ground displacements</li> </ul>

### 3.3 Survey areas

Figure 2 shows the survey areas in Nishiaraya and Tsurugaoka Districts of Uchinada Town where the ground failures were intensively identified and the displacements were measured. The survey area for the Nishiaraya District includes parts of the Miyasaka District and Muro District, where severe damage has been observed. Similarly, the survey area for the Tsurugaoka District includes parts of the Mukaiawagasaki District and Oonebu District.

This figure also shows the control points assumed not to be displaced. A main task of measuring the liquefaction-induced ground displacements is the determination of control points for common coordinates in pre- and post-earthquake aerial photogrammetry. Therefore, their locations shall be generally selected from points on mountainous terrain or plateaus where the ground is relatively stable, or from points on solid structures where there is no possibility of displacement. The horizontal and vertical control points in the survey were selected on the top of the sand dunes, which is considered unaffected by liquefaction. Complementary control points were also selected in the low-lying reclaimed land to support elevation setting for photogrammetry. The coordinates of the selected control points were obtained from the topographic map (1) in Table 1.

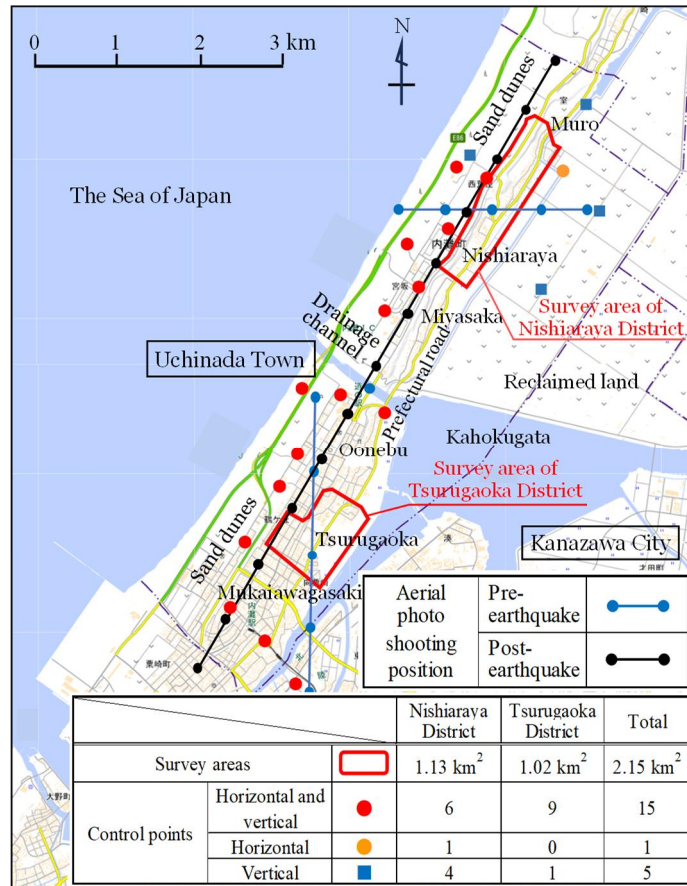
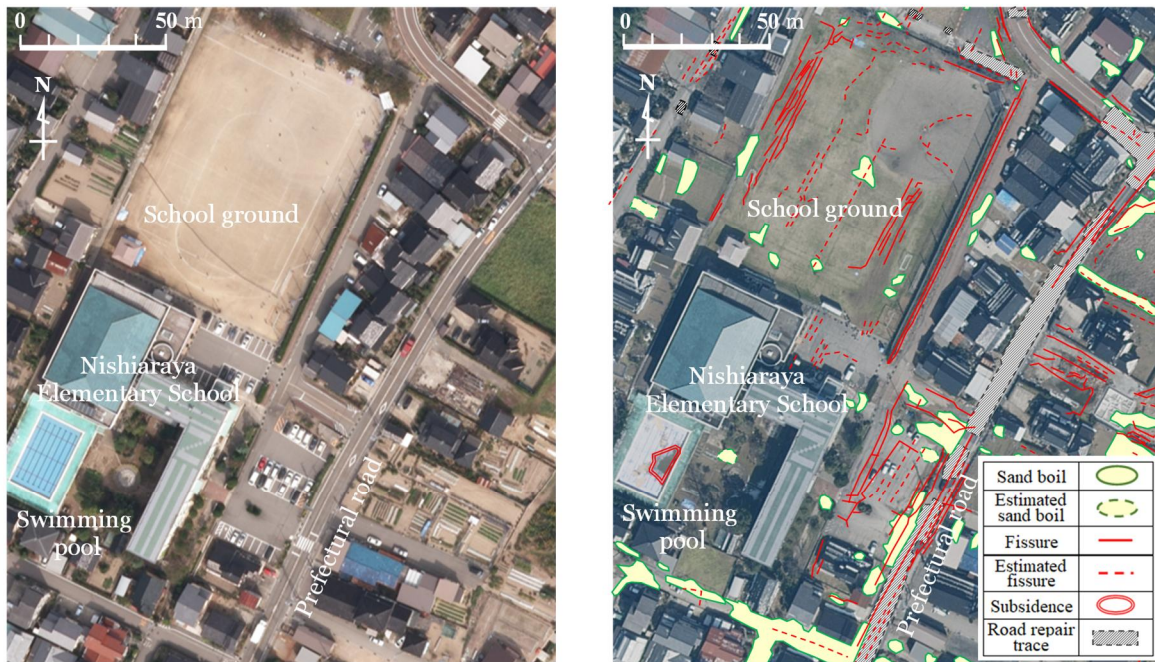


Fig. 2 Survey areas<sup>1)</sup>



(a) Pre-earthquake aerial photograph (taken in 2012)<sup>1)</sup>

(b) Post-earthquake aerial photograph (taken on March 11, 2024)

Fig. 3 Aerial photographs of the section around Nishiaraya Elementary School<sup>1)</sup>

## 4. IDENTIFICATION OF GROUND FAILURES AND MEASUREMENT OF DISPLACEMENTS

### 4.1 Ground failures

Ground failures such as sand boils, fissures, subsidence, uplift and sinkholes were identified by comparing the pre-earthquake aerial photos shown in (2) or (3) with the post-earthquake aerial photos shown in (5) in Table 1. Figure 3 shows aerial photos of the section around Nishiaraya Elementary School pre- and post-earthquake. As shown in Fig. 3(b), post-earthquake, numerous fissures and sand boils can be seen on the school ground. However, the post-earthquake photos used for identification were taken 70 days after the earthquake, many of the failures on Ishikawa Prefectural Route No.8 (Matto-Unoke Line) and others had already been repaired before the survey. Therefore, identification of ground failure in this section was based on sand boils and fissures. In Fig. 3(b), a single sinkhole was identified at an elementary school pool, based on damage observed on part of the pool bottom. Next, the locations and extents of these ground failures were transferred onto the topographic maps of the Nishiaraya and Tsurugaoka Districts in (1) in Table 1 to create ground failure maps for each section.

Figure 4(a) shows ground failures around Nishiaraya Elementary School. The section between steep slope and irrigation channel is gently sloping. The direction of the slope is perpendicular to the dune ridge lines and is also nearly perpendicular to the prefectural road and irrigation channel. The ground failures in Nishiaraya District occur mainly on the gently sloping section. There are several zones within the gently sloping section where ground failures are frequently observed, and among them, they are particularly concentrated around Nishiaraya Elementary School. As the general trend of ground failures is that more fissures occurred above the gently sloping section, and more sand boils occurred below the gently sloping section and in some reclaimed land. Numerous fissures are visible on the school ground of Nishiaraya Elementary School and the surrounding section, extending in the direction perpendicular to the slope. This suggests that tensile strains were caused by the ground moving along the slope.

A long series of fissures can be seen on the shoulder of the steep slope in the figure. These fissures were probably caused by a landslide due to seismic ground motion. A control point is located west of this position, but since it is about 300 m away, it was considered acceptable to treat it as fixed.

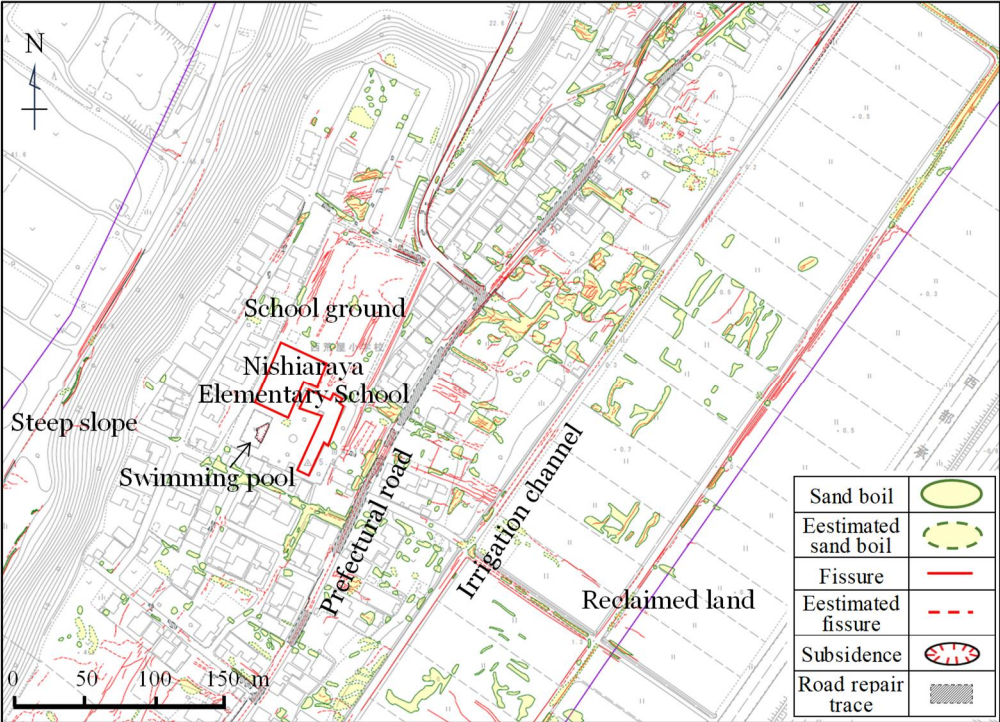
Figure 4(b) shows ground failures around Tsurugaoka Elementary School, including Uchinada Junior High School and Uchinada Town General Sports Ground. This section is also gently sloping. As in Nishiaraya District, the direction of the slope is nearly perpendicular to the prefectural road. The figure shows that ground failures in Tsurugaoka District occur less than in Nishiaraya District. However, there are zones where ground failures are concentrated in residential sections east of the prefectural road and around the Uchinada Town General Sports Ground.

### 4.2 Ground displacements

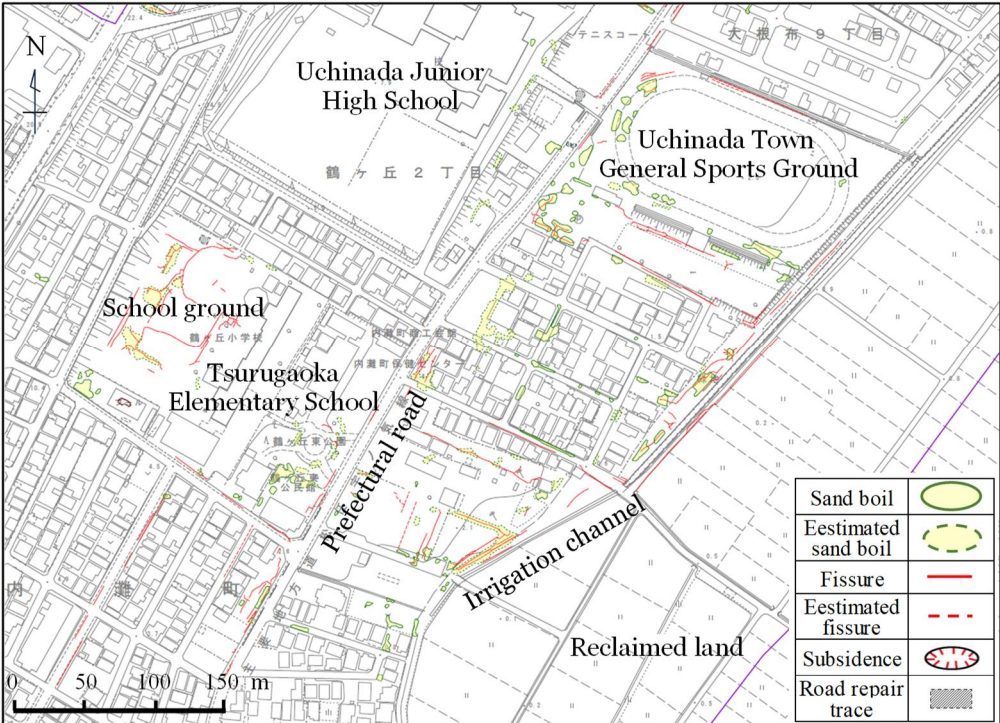
A total of 665 observation points were selected for displacement measurement, with 360 in Nishiaraya District and 305 in Tsurugaoka District. Observation points were selected mainly from manhole covers, corners of drainage pits, white lines on road surface markings, at the foot of telegraph poles, lighting poles, fences, and guardrail posts, corners of retaining walls, plantings, boundary walls, farmlands and building roofs, and points on bridges. 3D coordinates of the observation point pre- and post-earthquake were measured by aerial photogrammetry. Displacements in the X (east–west), Y (north–south), and Z (vertical) directions were obtained as the differences between the post-earthquake and pre-earthquake coordinates. The composed magnitudes of horizontal displacements were calculated from the displacements in the X and Y directions.

Table 2 shows the accuracies of displacement measurements. The standard deviations of control point coordinate residuals—defined as the standard deviations of the differences between the coordinates from topographic maps and survey results—were used as accuracy indicators for aerial photogrammetry. Next, as displacement was calculated from the coordinates of observation points pre- and post-earthquake, the accuracies of displacement measurement were determined using the law of error propagation.

The accuracies of horizontal displacement were estimated as about  $\pm 15$  cm in both districts. The accuracy of vertical displacement was estimated as  $\pm 8$  cm in Nishiaraya District, while it was as large as  $\pm 30$  cm in Tsurugaoka District.



(a) Around Nishiaraya Elementary School



(b) Around Tsurugaoka Elementary School

Fig. 4 Ground failures<sup>1)</sup>

Table 2 Accuracies of displacement measurement<sup>1)</sup>

		Nishiaraya District		Tsurugaoka District	
		Horizontal	Vertical	Horizontal	Vertical
Standard deviations of control point coordinate residuals	Pre-earthquake	±0.121 m	±0.035 m	±0.145 m	±0.300 m
	Post-earthquake	±0.079 m	±0.077 m	±0.079 m	±0.077 m
Accuracies of displacement measurement		$\pm\sqrt{0.121^2 + 0.079^2}$ = ±0.144 m	$\pm\sqrt{0.035^2 + 0.077^2}$ = ±0.084 m	$\pm\sqrt{0.145^2 + 0.079^2}$ = ±0.165 m	$\pm\sqrt{0.300^2 + 0.077^2}$ = ±0.309 m

Figure 5 shows ground displacements and ground failures around Nishiaraya Elementary School. It is arranged so that the downward slope of the ground surface is on the right side of the figure. Horizontal displacement directions are shown as vectors, with their magnitudes indicated alongside. Vertical displacements are shown in parentheses. The unit of displacement is cm. Positive magnitude for vertical displacement shows uplift, and negative magnitude shows subsidence. The figure shows that horizontal displacements occur on the gently sloping section between steep slope and irrigation channel, where numerous fissures and sand boils are observed. The direction of horizontal displacements generally follows the direction of the ground surface gradient (right direction in the figure). The maximum horizontal displacement in the section shown in Fig.5 is 3.1 m. On the other hand, the horizontal displacements in Tsurugaoka District are generally small, corresponding to the lower frequency of ground failures. However, in the residential section east of the prefectural road, an observation point showed a displacement of 0.9 m, and the authors confirmed many houses suffered damage such as subsidence and inclination, through field surveys.

## 5. CONSIDERATION OF GROUND DISPLACEMENT

Figure 6 shows the horizontal displacement components in the direction of each line at observation points near the lines in Fig. 5, together with the topographic cross-section along the line 2–2'. The figure shows that horizontal displacements start at the foot of the steep slope, increase near the center of the gently sloping section, and slightly decrease around the prefectural road. These displacements also extend to the irrigation channel at the boundary of the flat reclaimed land, where these almost converge. As shown in Figs. 6(a) and 6(b), “Upper section” and “Lower section” are zones with relatively small displacement, and “Central section” are zones with relatively large displacement. Looking at the maximum displacement in the Central section of each line, it is 3.1 m from the line 1–1', 2.6 m from the line 3–3', while it is relatively small at 2.1 m from the line 2–2'. Because the line 2–2' crosses the elementary school building, it is considered that the ground displacements were controlled by the foundation piles of the building.

## 6. COMPARISON OF GROUND DISPLACEMENT WITH PREVIOUS EARTHQUAKES

In previous studies<sup>13), 14)</sup> on ground displacement due to liquefaction in Niigata City, caused by the 1964 Niigata Earthquake, and in Noshiro City, caused by the 1983 Nihonkai-Chubu Earthquake, ground failures were identified and ground displacements were measured based on pre- and post-earthquake aerial photos. It was concluded that the main factors contributing to the ground displacement were the ground surface gradient and the thickness of the liquefied layer. These studies measured displacements based on differences in 3D coordinates from pre- and post-earthquake aerial photographs, using the same method as in this survey. Following these studies, we analyzed ground displacement trends around Nishiaraya Elementary School and compared them with the trends from previous earthquakes. Therefore, following the same procedure as in previous studies<sup>13), 14)</sup>, the lines were divided into sections, and the average horizontal displacements and average ground surface gradients were calculated for each section.

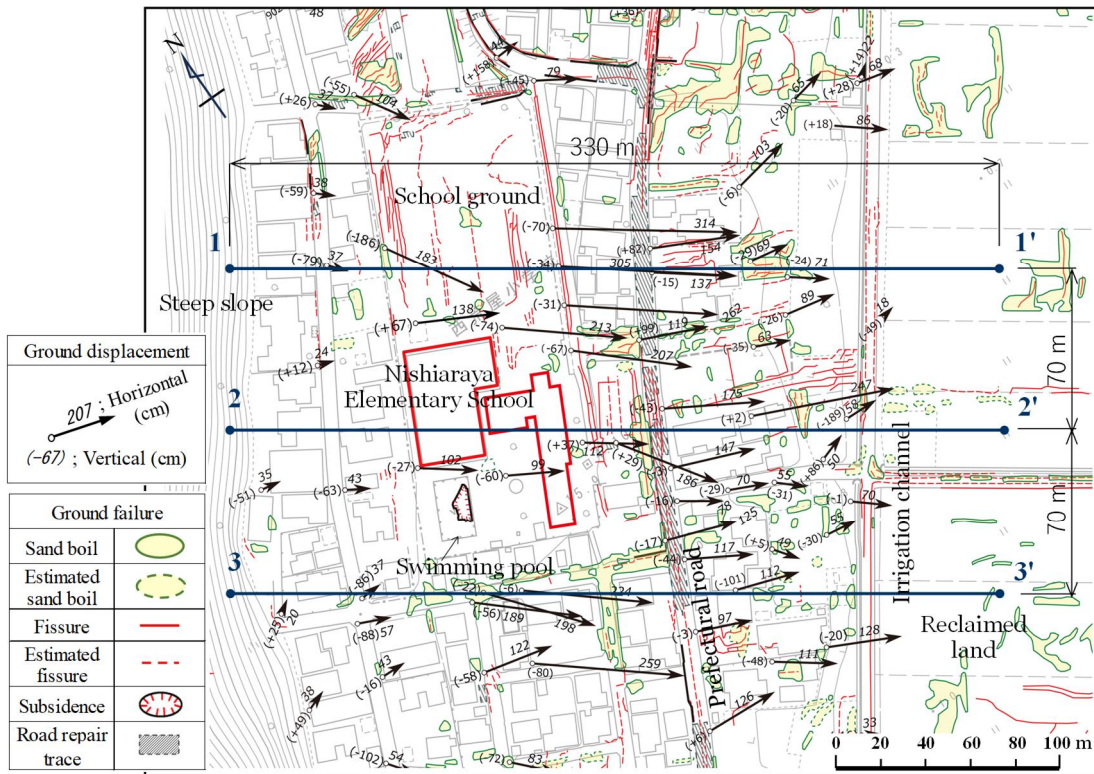
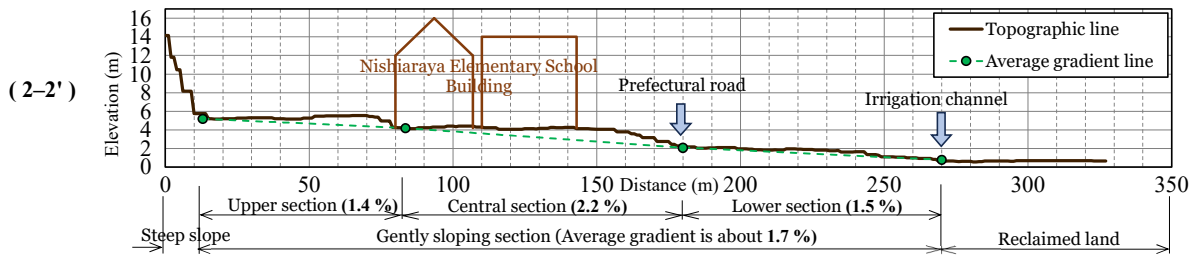
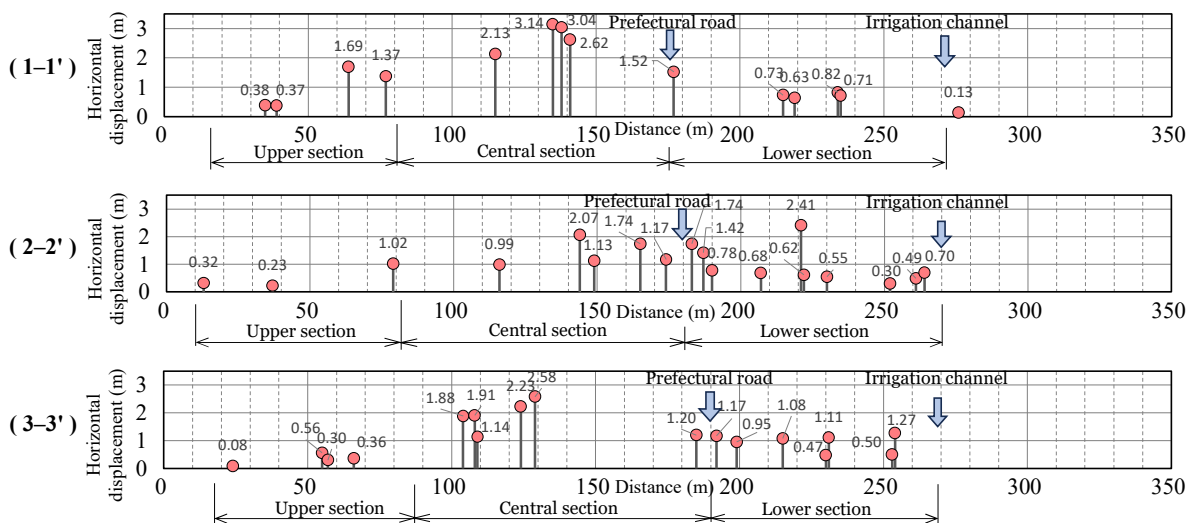


Fig. 5 Ground displacements and ground failures around Nishiaraya Elementary School<sup>1)</sup>



(a) Topographic cross-section along the line 2-2'



(b) Horizontal displacements along the line 1-1', 2-2' and 3-3'

Fig. 6 Topography and horizontal displacements around Nishiaraya Elementary School

Figure 7 shows the relationship between average horizontal displacement and average gradient for liquefied ground based on previous studies<sup>13), 14)</sup>, with the data from around Nishiaraya Elementary School (labeled as “Uchinada”) plotted on the same graph. Note that only the horizontal displacement data from the Central section were used, since the displacements in the Upper and Lower sections were small. The average horizontal displacement is the mean of the horizontal displacements within the Central section. The figure shows that the displacements in Uchinada Town were smaller than those of Niigata City, but were equivalent to those of Noshiro City.

Figure 8 shows the boring log at Nishiaraya Elementary School. The groundwater level at this site is shallow as GL-2.1 m. The N-values of the layer from the ground surface to GL-15.0 m range from 3 to about 10 (loose to medium compaction), and the layer is composed of fine sand with nearly uniform grain size. Below GL-15.0 m, fine sand with uniform grain size is deposited, with N-values ranging from 11 to 27 (medium to dense compaction). Therefore, the ground in this section is liquefiable in conditions of groundwater level, degree of compaction, and grain size composition.

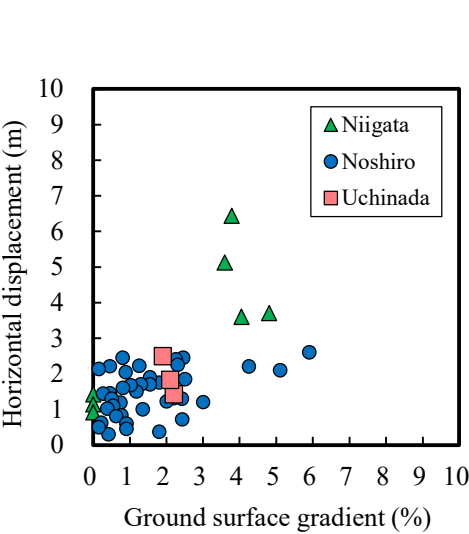


Fig. 7 Relationship between horizontal displacement and ground surface gradient<sup>1</sup>

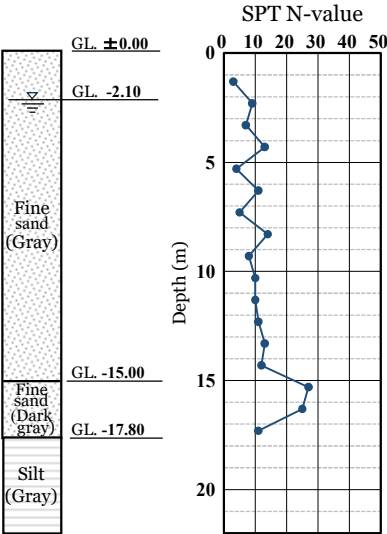


Fig. 8 Boring log at Nishiaraya Elementary School<sup>2</sup>

**7. CONCLUSIONS**

The Noto Peninsula Earthquake, due to ground motions with few precedents in the past, caused liquefaction-induced ground displacements on the east side of the dunes in Uchinada Town. Ground failures such as sand boils, fissures, subsidence, and uplift occurred on the ground surface. As a result, road pavements were impassable due to fissures, subsidence, and uplift, buried lifeline pipes were lost functionality for extended periods due to deformation and damage, and numerous residential buildings suffered subsidence, inclination, and collapse. Damage was particularly severe in Nishiaraya District in the northern area of the town. There, a maximum horizontal displacement of 3.1 m was observed around Nishiaraya Elementary School. Tsurugaoka District in the southern area, displacements were relatively smaller than in Nishiaraya District. However, in the residential section east of the prefectural road, an observation point showed a displacement of 0.9 m, and many houses did suffer damage, including subsidence and inclination. The reason why the damage in the northern area was greater than that in the

<sup>1</sup> Figure 7 is an edited version of Fig. 4 in Reference 14), pp. 224, with the addition of data from this survey.

<sup>2</sup> Figure 8 is based on the investigation results from soil boring NO. R6-07-B1 conducted by the Ministry of Land, Infrastructure, Transport and Tourism (provided by Uchinada Town Office).

southern area can be due to the difference in topography and ground conditions between the two areas. In particular, the northern area was lower in elevation due to soil excavation from land reclamation projects, and the groundwater level was closer to the surface. As a result, it is presumed that the area became more liquefiable than before.

This survey provides useful information for predicting liquefaction damage and proposing countermeasures during major earthquakes. We need to find the main problems in this field and work on solving them.

The Noto Peninsula Earthquake occurred on January 1, 2024, and the restorations were significantly delayed. Subsequently, in September of the same year, heavy rains hit Oku-Noto Region. The rains became a compound disaster, as they made the damage worse due to loosened ground, fissures, and other related factors on slopes that had collapsed during the earthquake. We extend our sympathy to everyone in the disaster-affected area.

## ACKNOWLEDGMENT

We thank Professor Emeritus Kenji Ishihara of the University of Tokyo, Professor Emeritus Masakatsu Miyajima of Kanazawa University, and Assistant Professor Masataka Shiga of Nagaoka University of Technology for providing valuable resources and advice during this survey. We thank the Uchinada Town Office for kindly allowing us to use their topographic maps and geotechnical data such as soil boring logs. We thank Mr. Iwao Yasuda, and Mr. Tatsuyuki Takano and Mr. Sanshiro Ohtake of Hasshu Co., Ltd. for their efforts in taking post-earthquake aerial photos and creating ground failure maps and ground displacement maps. We would like to express our sincere gratitude to all of them.

## REFERENCES

- 1) Institute for Disaster Mitigation of Industrial Complexes, Kanagawa, Japan: The 2024 Noto Peninsula Earthquake: Measurement of Ground Failures and Displacements in Uchinada Town, Ishikawa Prefecture in Japan, 26 pp., 2024 (in Japanese).
- 2) Japan Meteorological Agency: Strong-Motion Observation Data, Earthquake in the Noto Region, Ishikawa Prefecture at 16:10 on January 1, 2024 (in Japanese, title translated by the authors). [https://www.data.jma.go.jp/eqev/data/kyoshin/jishin/2401011610\\_noto/index.html](https://www.data.jma.go.jp/eqev/data/kyoshin/jishin/2401011610_noto/index.html) (last accessed on September 15, 2024)
- 3) National Research Institute for Earth Science and Disaster Resilience: Strong-Motion Seismograph Networks (in Japanese, title translated by the authors). <https://www.kyoshin.bosai.go.jp/kyoshin/quake/> (last accessed on September 15, 2024)
- 4) Ishikawa Prefecture Office: Human and Structural Damage Caused by the 2024 Noto Peninsula Earthquake (in Japanese, title translated by the authors). [https://www.pref.ishikawa.lg.jp/saigai/documents/higaihou\\_193\\_0306\\_1400.pdf](https://www.pref.ishikawa.lg.jp/saigai/documents/higaihou_193_0306_1400.pdf) (last accessed on March 6, 2025)
- 5) Ishikawa Prefecture Office: Fundamental Land Classification Survey: Tsubata, 43 pp., 1985 (in Japanese).
- 6) Economic Planning Agency: Fundamental Land Classification Survey: Kanazawa, 126 pp., 1969 (in Japanese).
- 7) Fuji, N.: The Coastal Sand Dunes of Hokuriku District, Central Japan, *The Quaternary Research*, Vol.14, No.4, pp.195–220, 1975 (in Japanese).
- 8) Imperial Land Survey of Japan: Topographic Map: Tsubata, 1st ed., 1930 (in Japanese).
- 9) Imperial Land Survey of Japan: Topographic Map: Awagasaki, 1st ed., 1930 (in Japanese).
- 10) Uchinada Town Office: Urban Planning Base Map, 2016 (in Japanese).
- 11) Geospatial Information Authority of Japan: Aerial Photographs (Nishiaraya District), 2012 (in Japanese).
- 12) Geospatial Information Authority of Japan: Aerial Photographs (Tsurugaoka District), 2007 (in Japanese).

- 13) Hamada, M., Yasuda, S., Isoyama, R. and Emoto, K.: Observation of Permanent Ground Displacements Induced by Soil Liquefaction, *Journal of Japan Society of Civil Engineers*, Vol. 376, 3–6, pp. 211–220, 1986 (in Japanese).
- 14) Hamada, M., Yasuda, S., Isoyama, R. and Emoto, K.: Study on Liquefaction-Induced Permanent Ground Displacements and Earthquake Damage, *Journal of Japan Society of Civil Engineers*, Vol. 376, 3–6, pp. 221–229, 1986 (in Japanese).

**(Original Japanese Paper Published: August, 2025)**  
**(English Version Submitted: October 14, 2025)**  
**(English Version Accepted: December 23, 2025)**